

Effect of drainage discs on the condensing heat transfer performance of vertical fluted tubes

H. Gökçe, C. Özgen and T. G. Somer*

Heat transfer characteristics of fluted tubes with drainage discs were determined by a pilot-plant study. To find the effect of drainage disc spacings on the condensing heat transfer coefficient, spacings of 5, 10, 15 and 20 cm were used. The Wilson-plot technique was used in the evaluation of experimental data. The results showed that, for the tested disc spacing (5–20 cm) and heat flux ranges (60 000–100 000 W/m²), condensing heat transfer coefficients for steam were higher by a factor of about 1.5–3.0 than those for a fluted tube without discs and by a factor of about 3.5–6.7 than those for a smooth tube. The experimental results were also to check the validity of an improved semi-empirical hydrodynamic model originally developed by Özgen and Somer. The results were in good agreement, with a maximum deviation of $\pm 16\%$.

Keywords: *drainage discs, fluted tubes, condensation, heat transfer*

Introduction

Among the many methods for increasing condensation heat transfer¹ is the enhancement of the heat transfer coefficient by using modified heat transfer surfaces such as double-fluted tubes, which is the subject of this study.

The fluted tubes profile was first proposed by Gregorig² in 1954. In these tubes, the curvature difference of the sinusoidal profile of the tube wall on the plane perpendicular to the tube axis develops pressure differences in the condensate film due to surface tension forces. In vertical fluted tube condensers, the condensate forming on the outer surface of the tube drains from the crests to the grooves of a fluted as a result of surface tension forces, leaving bare areas over the crests. The condensate accumulating in the grooves flows in the vertical direction by gravity. This film thinning over the crests to the grooves of a flute as a result of surface and thus increases the average condensing film coefficient in comparison with a smooth surface. However, the fluted tubes show reduced heat flow in the lower sections of the tube length, as a result of increase in film thickness as the amount of condensate increases. When the grooves are filled with condensate, the fluted tube behaves in a similar way to a smooth tube. Therefore, a modification must be made to prevent the increase of film thickness in the grooves of a fluted tube after a certain length. Some studies^{3,4} of fluted tubes with circular drainage discs (Fig 1) for ammonia and R-113 condensation have been made.

Combs³ has evaluated the performance of fluted tubes with ammonia condensing on the outside. After testing the performance of equally spaced drainage discs

with effective condensing length of 0.15 m, he has shown that there is no appreciable advantage in using lesser drainage disc spacings in the range of heat fluxes 5000–50 000 W/m².

Mori *et al*⁴ have analytically and experimentally studied the effect of condensation length on the rate of heat transfer. They examined several fluted shapes and tube lengths with R-113 condensing on the outer surface of the tubes, and concluded that the optimum disc spacing is less than 0.1 m not only for R-113 but also for water.

Experimental set-up and procedure

A schematic diagram of the pilot plant is shown in Fig 2. It consisted of a concentric pipe heat exchanger, coolers, water preheater, steam desuperheater and auxiliary equipment. The heat exchanger, which consisted of a single fluted tube at the centre, surrounded by a galvanized steel jacket, was mounted in a vertical position. Steam entered at two points on the jacket where baffles had been installed to prevent sudden impact of steam and the impingement of possible entrainment on the fluted tube surface. Steam pressure and temperature were measured before and after the entrance to the jacket. Cold water entered from the top, providing a parallel flow. Although the steam was saturated, it was considered essential to eliminate possible superheat and impurities, such as oil drops and solids, before this steam entered the exchanger. A hot-water tank was used as a desuperheater and cleaner in which steam dispersed into fine bubbles and rose to the surface. Desuperheated steam passed through an entrainment separator, then entered a calorimeter, the vessel of which served also to dampen pressure fluctuations in the steam lines. Considering that the errors due to 'gas' (air) could be large, in all experiments steam pressure was kept a few millimetres Hg

* Chemical Engineering Department, Middle East Technical University—ODTÜ, Ankara, Turkey
Received 11 June 1985 and accepted for publication in final form on 24 February 1986

above the atmospheric pressure. This provided a steady flow of steam through the system and allowed discharge of non-condensibles at frequent intervals through a vent line mounted on top of the exchanger, thus preventing chances for accumulation.

The experimental set-up did not include any 'dump condenser', and the condensate forming on the fluted tube at the centre was drained and discharged automatically by means of a steam trap installed at the lowest point of the jacket of the heat exchanger. During a normal run, the trap would open and discharge the condensate at approximately 45-second intervals. Thus there was no appreciable condensate accumulation inside the heat exchanger. The condensate was further cooled in a double-pipe heat exchanger. It was collected in a vessel and measured periodically for the heat balance calculations.

Distilled water was pumped from a storage tank through a water preheater before it entered the exchanger. The function of the preheater was to heat the water before each experiment to a preset level and also to control inlet temperature of water. Water discharging from the exchanger was cooled and recycled for re-use. Temperatures were measured with resistance thermometers accurate to $\pm 0.01^\circ\text{C}$. The outer surface temperatures of the fluted tubes were measured at six equal height intervals by mineral-insulated iron-constantan thermocouples with an accuracy of $\pm 0.1^\circ\text{C}$.

The fluted tube tested was made of a special alloy with the composition 76% Cu, 2% Al, 0.4% As and 21% Zn. It was supplied by Yorkshire Imperial Metals Ltd and

had the trade name of 'Yolcabro'. Specifications of the tested fluted tube are given in Table 1.

Experiments were performed with different drainage disc spacings in order to observe the tube length effect on the rate of condensation heat transfer. In practice, drainage discs are made of neoprene³. However, in the present study, the drainage discs used were made of galvanized sheet iron of thickness 0.5 mm. Inside and outside diameters of the discs were 50.8 and 87.5 mm, respectively. A small inclination was given to the disc shape to provide drainage of the condensate easily from the tube surface (Fig 3). Discs were attached to the outside surface by an industrial glue. After each set of runs, it was observed that the discs were still firmly attached to the surface, and the glue was not affected by the presence of steam.

Experiments were performed at atmospheric pressure. The flow rate of circulating water was varied in order to obtain data for the Wilson-plot technique⁵. For the application of this method, water had to be recirculated inside the tube at a high rate to maintain low temperature rise. The inlet water temperature was kept at 88.5°C (361.5 K). It was ensured that the temperature of steam, water and the fluted tube surface remained constant for a period of at least 30 min before the readings were taken.

On the jacket of the heat exchanger there were no observing glasses, hence the tubes could not be viewed and the possibility of dropwise condensation, which could cause large errors in the calculations, could not be directly ruled out. Nevertheless, it is well known that as

Notation			
a	Radius of curvature of condensate film surface	U	Overall heat transfer coefficient
a_0	Radius of curvature of a groove section	\dot{V}	Volumetric flow rate
A	Flow area of fluid	$\Delta\dot{m}$	Condensation rate
A_i, A_o	Inside and outside heat transfer areas of tube	ΔT	Temperature difference
A_w	Mean heat transfer area of tube	ΔT_{\ln}	Log-mean temperature difference
b_0	Radius of curvature of crests	ΔX_w	Tube wall thickness
C_p	Heat capacity	Δz	Interval of tube length
C_i, C_o	Coefficients in Eqs (14) and (15)	α	Flute angle
D	Tube diameter	γ	Constant in Wilson-plot $\equiv \frac{\rho_f^2 g \lambda k_f^3 A_o}{\mu_f L_T}$
g	Gravitational acceleration	$\bar{\delta}$	Average film thickness over the crests
h	Condensate film thickness	θ, θ_1	Angles facing condensate film surface
\bar{h}	Average film thickness in groove section	θ_2	$\pi/2 - \alpha$
h_i, h_o	Water side and condensing side heat transfer coefficients	λ	Latent heat of condensation
H	Maximum film thickness	μ	Viscosity
k	Thermal conductivity	ρ	Density of water
L	Length of tube	σ	Surface tension
L_1	Length of thin film section		
\dot{m}	Condensate mass rate	Subscripts	
N	Number of flutes	D	Refers to discs
Pr	Prandtl number $\equiv C_p \mu / k$	f	Properties to be evaluated at film temperature
Re	Reynolds number $\equiv Dv\rho/\mu$	i	Inside
p	Pitch of flutes	n	Interval number
P	Perimeter of tube	o	Outside
Q	Heat load	T	Refers to total
s	Arc length	w	Wall
S_T	Total length of one flute		

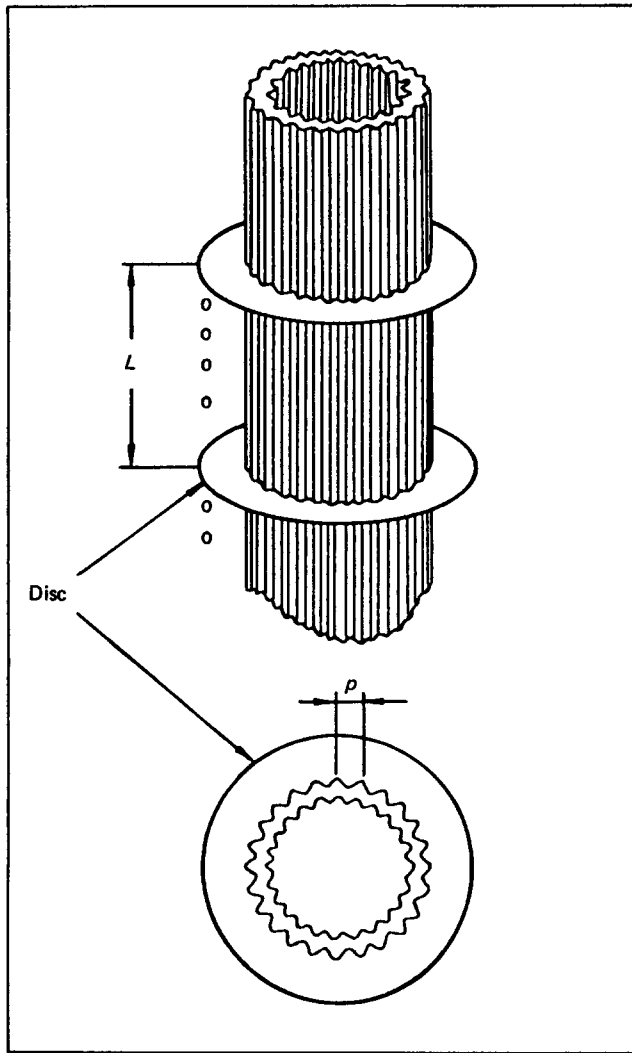


Fig 1 Vertical fluted tube with drainage discs

long as organic film-forming substances are eliminated from the steam and the surface of the tubes are not precoated with a noble metal, after a sufficient length of continuous operation the chances for dropwise condensation are extremely small—in fact, non-existent. Therefore, the test fluted tubes were thoroughly cleaned before the experiments, and the reproducible data were only obtained after several days of operation. After the experiments, when the tubes were dismantled it was observed that the tubes were covered by a very thin, hardly noticeable oxide film. Distilled water droplets were spread almost immediately on these oxide films. There was no oil or organic contaminants, as observed under a magnifier. The primary cause of failure in dropwise condensation is the contamination of the surfaces by metal oxides. A very good surface providing dropwise condensation can be contaminated after a short time of study, on account of oxides. Therefore, we believe that only film condensation occurred over the fluted tubes.

The concentric-pipe heat exchanger, containing the industrial-size fluted tube under study, was fastened to the framework by rubber cushions and rings in order to

Table 1 Specifications of the fluted tube tested

Diameter D	50.8 mm
Number of flutes N	50
Plain thickness Δx_w	0.812 mm
Outside perimeter P_o	0.1972 m
Inside perimeter P_i	0.1922 m
Depth d	1.08 mm
Pitch p	3.19 mm
Length L	1.80 m
Radius of groove curvature a_0	0.4 mm
Radius of crest curvature b_0	0.8 mm
Flute angle α	45°
Total flute length S_T	3.945 mm

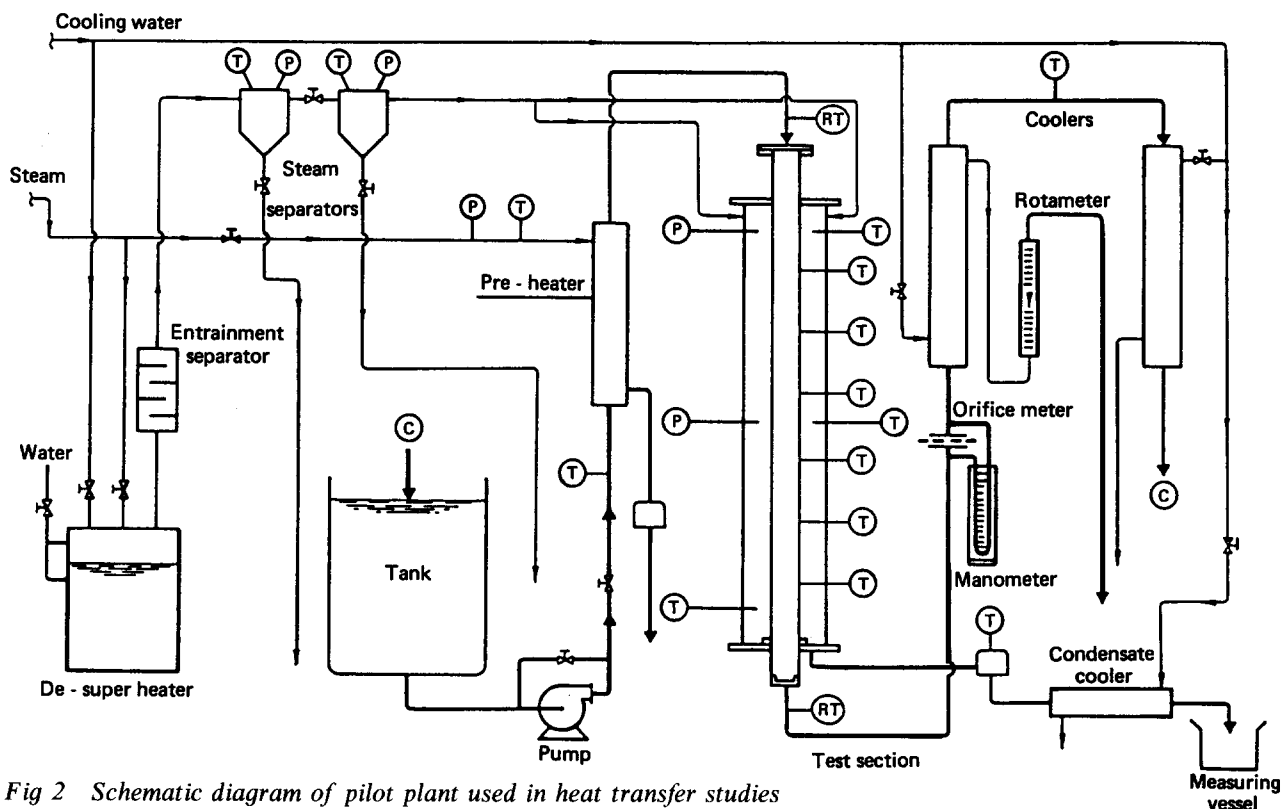


Fig 2 Schematic diagram of pilot plant used in heat transfer studies

eliminate the effects of vibration in the system. This was necessary to prevent additional surface rippling and turbulence of the liquid film condensate on the outer surface of the fluted tube.

The application of a hydrodynamic model

As a result of the hydrodynamic studies which have been carried out by Somer and Özgen⁶, one can determine the film thickness distribution of falling condensate films within a flute for a specific flow rate. Their model is based on photographs of the condensate profiles taken. After magnification of the photographs of condensate films, they have observed that the film thickness over the crests is hardly noticeable, while the condensate surface in the grooves, which is the liquid-vapour interface, is largely determined by the surface tension forces and can be approximated by a circular arc (Fig 4). The radius of this circle is reported to be a function of flute profile and condensate flow rate in the grooves. They have obtained

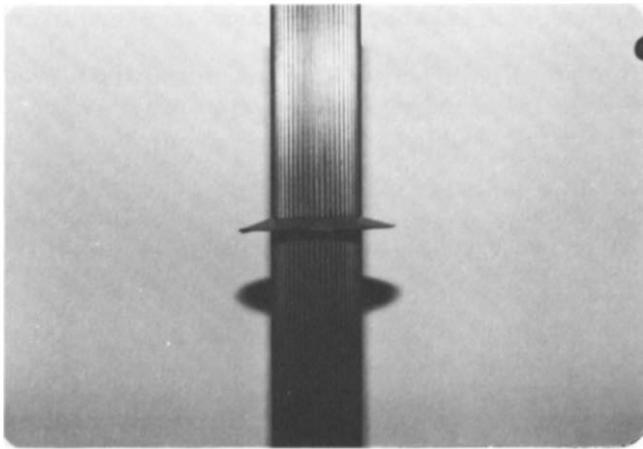


Fig 3 Fluted tube with drainage disc

relationships for calculation of the condensate flow rate in the grooves for a specific profile, and the average film thickness over the crests and the grooves.

The application of this hydrodynamic model to heat transfer was done by dividing the total tube length into n intervals. The length of each interval was taken as Δz . Then, the condensed amount $\Delta \dot{m}$ for each Δz can be calculated from

$$\Delta \dot{m} = \Delta \dot{m}_{\text{groove}} + \Delta \dot{m}_{\text{crest}} \tag{1}$$

According to the model, $\Delta \dot{m}$ is given by

$$\Delta \dot{m} = \frac{\Delta T \Delta z}{\lambda} k \left[2 \left(\frac{a \theta_2}{h} \right) + 2 \int_0^{L_1} \frac{ds}{\bar{\delta}} \right] \tag{2}$$

The average film thickness over the crests, $\bar{\delta}$, is given⁶ as

$$\bar{\delta} = 1.131 \left(\frac{k \Delta T \mu}{\lambda \rho \sigma} \right)^{0.25} \frac{L_1^{0.5}}{\left(\frac{1}{b_0} + \frac{1}{a} \right)^{0.25}} \tag{3}$$

Thus,

$$\Delta \dot{m} = \frac{\Delta T \Delta z}{\lambda} k \left[1.886 L_1^{0.5} \left\{ \frac{\rho \sigma \lambda}{k \Delta T \mu} \left(\frac{1}{b_0} + \frac{1}{a} \right) \right\}^{0.25} \frac{2 a \theta_2}{h} \right] \tag{4}$$

Starting from the bottom of the test tube, and knowing the condensate profile at a given condensate flow rate, the value of $\Delta \dot{m}$ for the n th interval can be calculated from Eq (4). The amount of the condensate leaving the interval number $(n - 1)$ can be found as

$$\dot{m}_{n-1} = \dot{m}_n - \Delta \dot{m} \tag{5}$$

and \dot{m}_n is defined as

$$\dot{m}_n = \dot{m} / N \tag{6}$$

where \dot{m} is the total condensate amount per unit time for the tested fluted tube and N is the number of flutes.

Proceeding similarly for the whole length of the

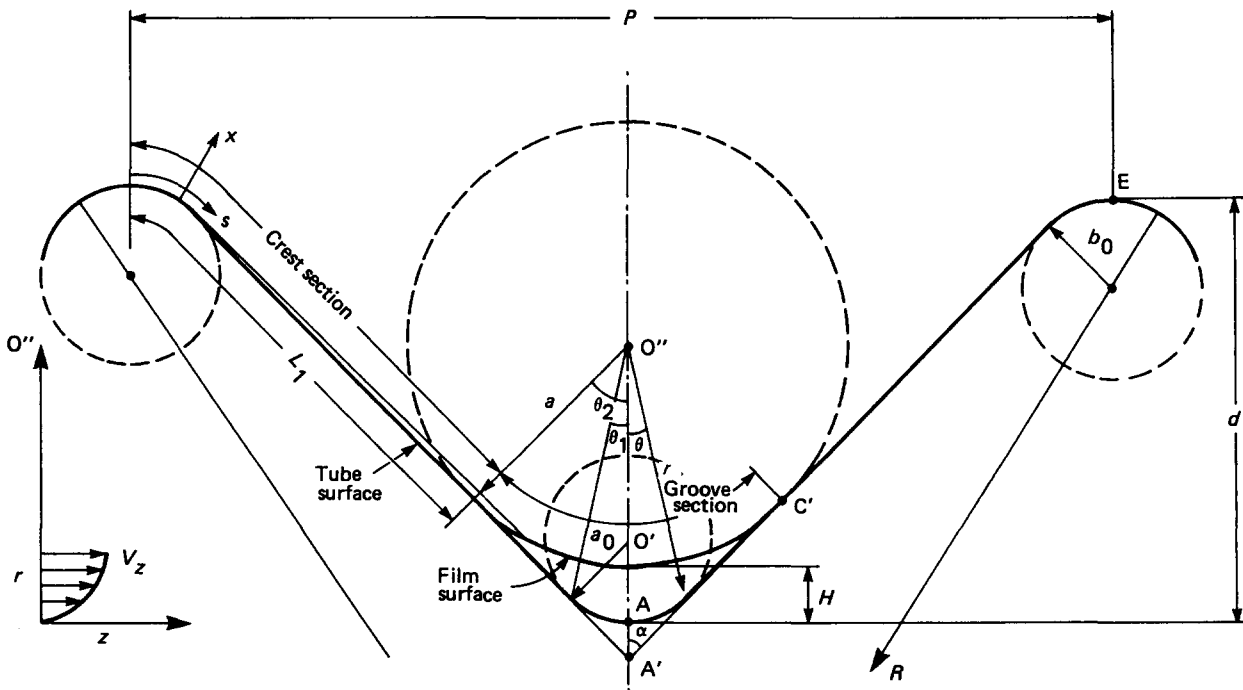


Fig 4 Condensate profile over a flute

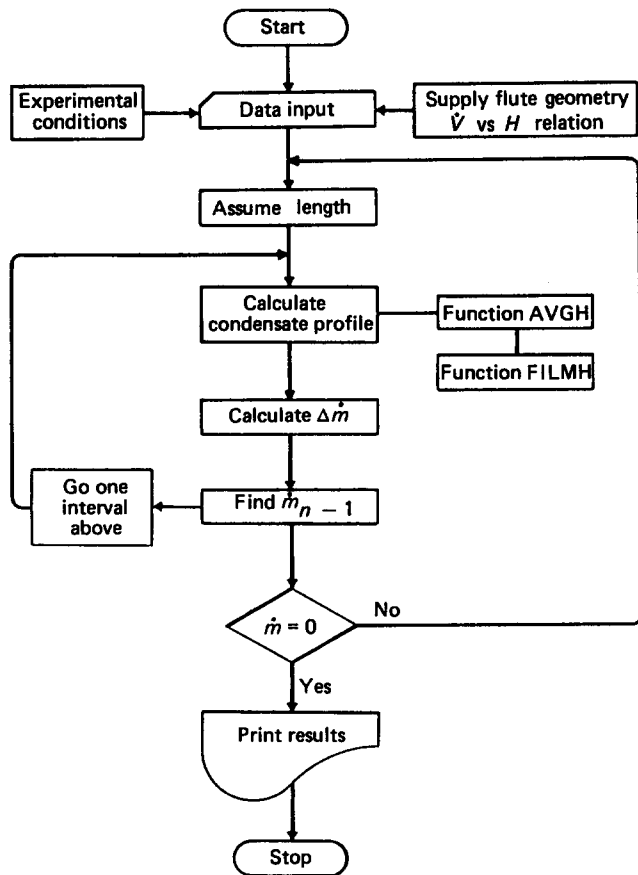


Fig 5 Algorithm for the application of the hydrodynamic model of Somer and Özgen⁶ to heat transfer

tube, the condensate flow rate is calculated for each interval. If the correct assumptions are made and if the model is good enough for the tested tube length, zero condensate rate must be found at the top of the tube. As a result of the above calculation, for any arbitrarily chosen condensation rate data the calculated tube length to obtain the same condensation rate over the tube can be smaller or larger than the actual tested tube length on which the data have been taken. A computer program was prepared to calculate the condensation length.

For computer application, some quantities must be analytically defined. Referring to Fig 4, the local film thickness h can be expressed as

$$h = a \left\{ \frac{1}{\cos(\theta_2 - \theta)} - 1 \right\} \quad \text{for } \theta_1 \leq \theta \leq \theta_2 \quad (7)$$

$$h = (a - a_0) \frac{\cos \theta}{\sin \alpha} - a + a_0 \left[1 - \left(\frac{a - a_0}{a_0} \right)^2 \frac{\sin^2 \theta}{\sin^2 \alpha} \right]^{0.5} \quad \text{for } 0 \leq \theta \leq \theta_1 \quad (8)$$

where

$$\theta_1 = \theta_2 - \tan^{-1} \left\{ \left(\frac{a - a_0}{a} \right) \cot \alpha \right\} \quad (9)$$

Other geometrical quantities are given as follows: the maximum film thickness,

$$H = (a - a_0) \frac{1 - \sin \alpha}{\sin \alpha} \quad (10)$$

the flow area of fluid,

$$A = (a^2 - a_0^2) (\cot \alpha - \theta_2) \quad (11)$$

the thin film flow length over the crests,

$$L_1 = \frac{S_T}{2} - (a - a_0) \cot \alpha + a_0 \theta_2 \quad (12)$$

The algorithm for the calculation of the condensation length is given in Fig 5. However, this procedure necessitates the relationship of volumetric flow rate as a function of maximum film thickness in the grooves. This relationship is obtained by curvefitting the experimental data by Özgen⁷. For the curvefitting of the data, Marquardt's regression method is used and the model equation (for the fluted tube tested) is found to be in the form

$$\dot{V} = 8.28 \times 10^{-7} H^{2.54} \quad (13)$$

where \dot{V} , volumetric flow rate, is in m^3/s and H is in mm. In the computerization of the hydrodynamic model, physical properties (k , σ , ρ , μ , λ), experimental conditions (\dot{m} , ΔT), flute geometry (a_0 , b_0 , α , θ_2 , S_T), and regression results (\dot{V} versus H) are given as inputs to the program. The condensate profile is found by using Eqs (7) to (12) for a given condensate rate, and then the calculated film thicknesses are used to find the average film thickness \bar{h} . The condensed amount $\Delta \dot{m}$, is later calculated by using Eq (4) for a condensation length of Δz . The next step is the calculation of condensate rate from the section $(n-1)$, and this is found from Eq (5). Proceeding in this way, a condensation tube length is calculated which gives a condensate rate of zero at the top. The calculated and the actual tube lengths are compared to find the error.

Results and discussion

The modified Wilson-plot technique enables one to calculate the outside and inside film heat transfer coefficients. The Wilson-plot drawings of experimental data are shown in Fig 6.

The reciprocals of the intercepts of the lines give the values of C_o , the coefficients in Eq (14) of outside heat transfer coefficient h_o , and the reciprocals of the slopes give the values of C_i , the coefficient in Eq (15) of inside heat transfer coefficient h_i :

$$h_o = C_o \left(\frac{\rho_f^2 g k_f^3 \lambda A_o}{\mu_f L_T Q} \right)^{1/3} \quad (14)$$

$$h_i = C_i Re_i^{0.795} Pr_i^y \frac{k_i}{D_i} \quad (15)$$

where $y = 0.495 - 0.225 \ln Pr_i$.

The values of inside coefficient were found to be almost uniform, while the outside heat transfer coefficient h_o varied with disc spacing as shown in Fig 7. In the modified Wilson-plot technique more accurate results can be obtained when data are taken to obtain smaller values for the abscissa in Fig 6, which decreases the amount of interpolation to find the intercept. This is possible by working at high Reynolds numbers, which enables one to obtain more accurate results, especially for C_o and h_o . This is one of the reasons why the experiments were performed at high Reynolds numbers. Also, the evaluated experimental data shown in Fig 6 or Fig 7 as a single point actually represent several repeated experiments done at the same conditions.

The variation with disc spacing of the coefficient C_o of the outside film coefficient is shown in Fig 8, which

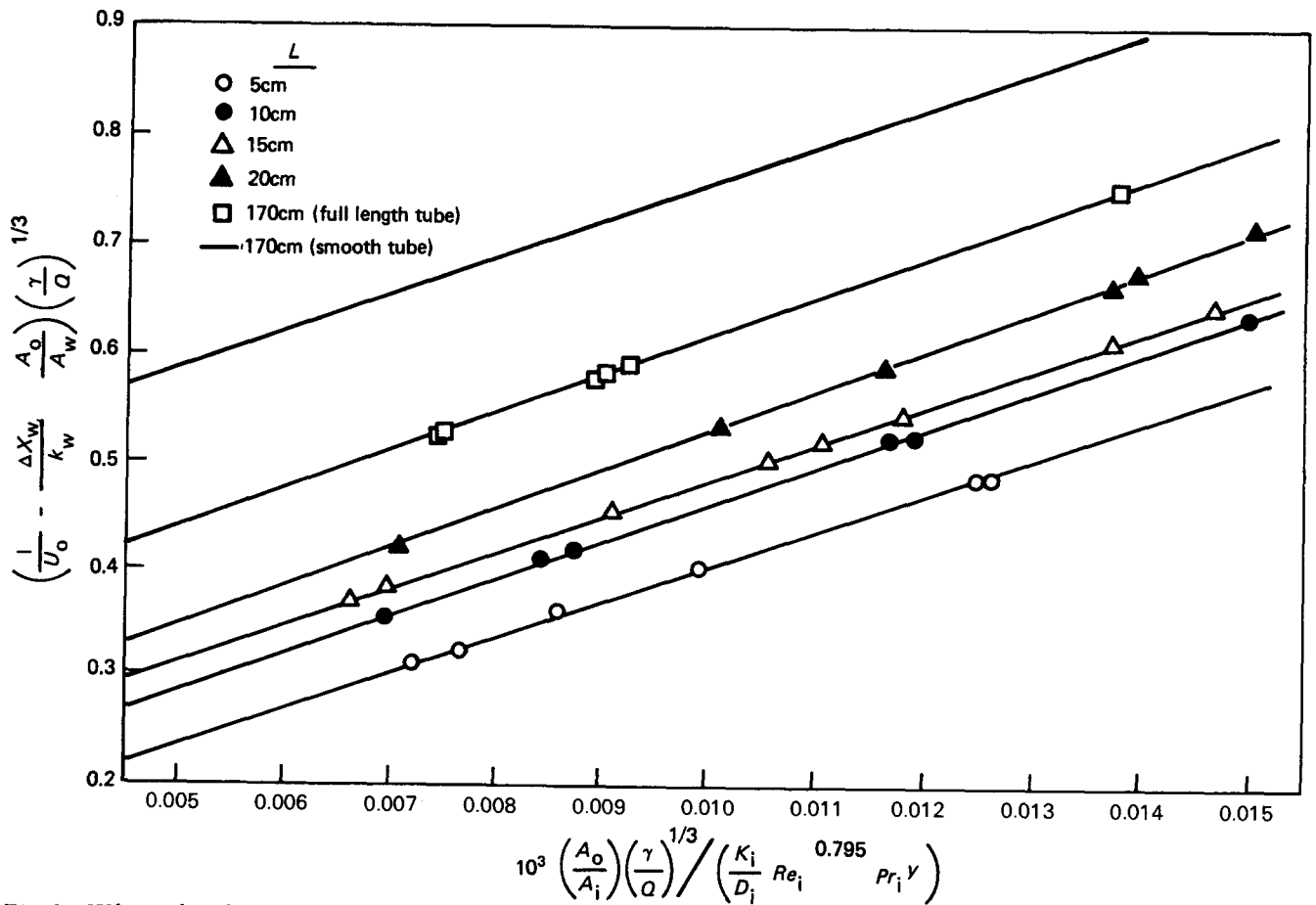


Fig 6 Wilson-plot for different disc spacings

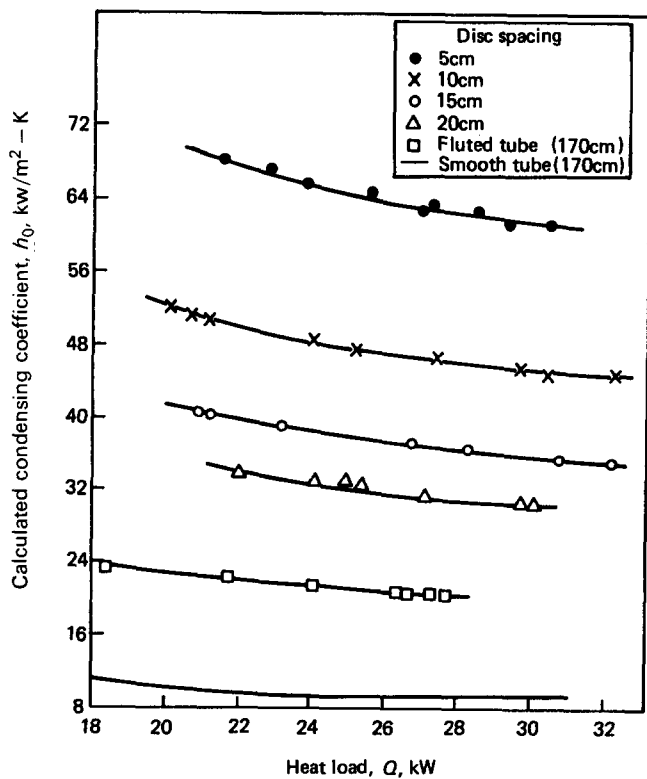


Fig 7 Comparison of heat transfer performances, h_o , versus Q , fluted tube for different disc spacings and for a smooth tube

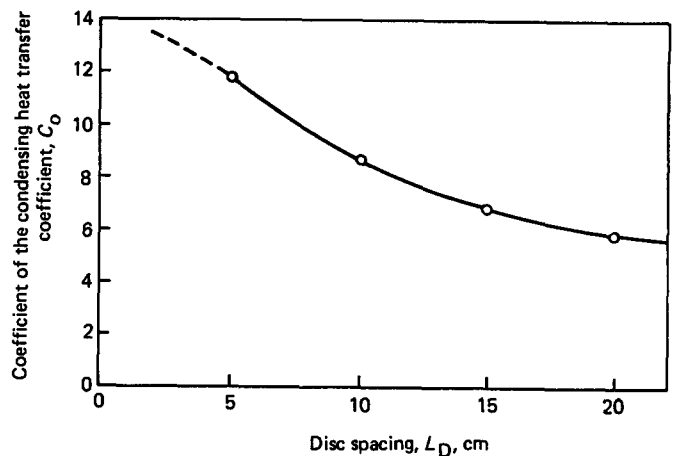


Fig 8 Variation of C_o with disc spacing

gives a good indication of the enhancement. The minimum disc spacing tested was 50 mm in this study, and it was observed that the appreciable enhancement in the heat transfer performance of the fluted tube was seen at disc spacings less than 100 mm. The enhancement obtained in this study was not observed by Combs³ since the minimum disc spacing he tested was 0.15 m. It must be noted that the improvement of tube performance by the addition of discs is strongly influenced by the flute geometry.

It can be seen from Fig 8 that C_o increases as disc

spacing L_D decreases. Therefore, one might think that, for shorter disc spacing, better heat transfer rate will be obtained. However, as disc spacing decreases, another factor, surface tension forces, plays a role in the formation of films over the fluted tube between discs.

As can be observed from Fig 9, for wider disc spacing (Fig 9(a)) a lot of vapour condenses on the tube surface, the groove in the lower part of the tube is filled up by condensate, and the condensing performance deteriorates. The addition of drainage discs (Fig 9(b)) causes the removal of this condensate from the surface to provide surfaces for high heat transfer rates. On the other hand, the tube with discs of shorter spacing has smaller average heat flux due to the effect of surface tension forces which create surface curvature of the condensate at the disc root. The condensate on the disc is pulled up along the grooves by surface tension forces and fills them, forming stationary pockets. Thus, the addition of the discs at shorter spacing increases the average film thickness over the tube surface, and the heat transfer performance of the fluted tube deteriorates. If a very short

spacing is used, the expected condensate profile will be as shown in Fig 9(c).

In order to find the optimum disc spacing, economic evaluations must be made. It is observed that, when more discs are used, heat transfer is increased. But the extra cost of additional discs must be equal to the gain in heat transfer at the optimum disc spacing. Different materials of construction and method of manufacturing can be used for discs, resulting in different costs. Therefore, the economic evaluations are left open and depend on various types of discs that can be used in different applications. Once the cost data are available, Fig 8 can be used to find optimum disc spacing. Nevertheless, it can be seen from Fig 8 that, by reducing tube lengths below 100 mm, heat transfer increases, showing the effect of condenser tube length on heat transfer.

In order to calculate the condensation lengths on fluted tubes with drainage discs, an improved hydrodynamic model was used. In application, equal condensation rates were assumed at each interval between discs. The calculated condensation length was compared with the actual disc spacing L_D . The final result of iterations is given in Table 2 for a disc spacing of 100 mm. In the test run given in Table 2 a total condensation rate of 8.37×10^{-3} kg/s was obtained. This gives a condensation rate per flute of $8.37 \times 10^{-3}/50 = 1.67 \times 10^{-4}$ kg/s-flute and at each disc spacing of $1.67 \times 10^{-4}/18 = 9.3 \times 10^{-6}$ kg/s-flute-interval.

Thus the theoretical condensation length was calculated to be 111.9 mm to give the same experimental condensation rate. Therefore, the error was 11.8%, which is tolerable for heat transfer studies. In the table, the calculated average film thickness \bar{h} , radius of condensate surface curvature a , maximum film thickness H and condensation at each interval Δz are also given. The interval Δz along the tube length is decreased in the upward direction where condensation rate is high, to reduce the error involved in assuming a constant film thickness \bar{h} , throughout the interval Δz .

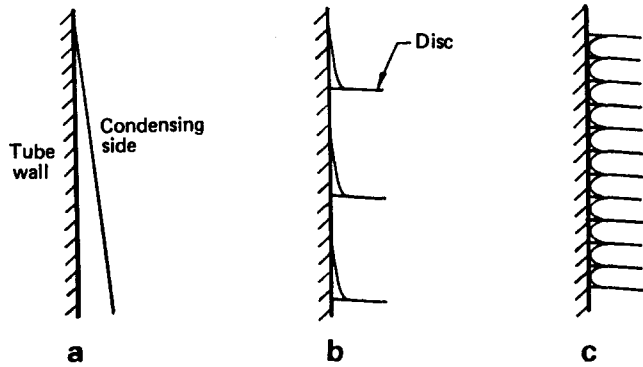


Fig 9 Effect of surface tension on the disc root: (a) wide disc spacing; (b) intermediate spacing; (c) close spacing

Table 2 Application of the improved hydrodynamic model to heat transfer

z (mm)	Condensation rate m . (kg/s-flute)	a (mm)	H (mm)	\bar{h} (mm)	$\Delta \dot{m}$ (kg/s-flute)
111.9	9.318×10^{-6}	0.0823	0.0175	0.0079	1.009×10^{-6}
99.5	8.818×10^{-6}	0.0805	0.0168	0.0077	0.925×10^{-6}
88.2	7.882×10^{-6}	0.0788	0.0161	0.0074	0.850×10^{-6}
77.9	7.031×10^{-6}	0.0771	0.0154	0.0072	0.780×10^{-6}
68.6	6.263×10^{-6}	0.0754	0.0147	0.0068	0.716×10^{-6}
60.2	5.544×10^{-6}	0.0738	0.0139	0.0066	0.656×10^{-6}
52.5	4.876×10^{-6}	0.0721	0.0133	0.0064	0.603×10^{-6}
45.5	4.275×10^{-6}	0.0705	0.0126	0.0065	0.553×10^{-6}
39.1	3.724×10^{-6}	0.0689	0.0119	0.0059	0.508×10^{-6}
33.1	3.223×10^{-6}	0.0673	0.0113	0.0056	0.466×10^{-6}
28.1	2.756×10^{-6}	0.0657	0.0106	0.0053	0.428×10^{-6}
23.3	2.321×10^{-6}	0.0640	0.0099	0.0050	0.392×10^{-6}
18.9	1.937×10^{-6}	0.0623	0.0093	0.0047	0.361×10^{-6}
15.0	1.570×10^{-6}	0.0606	0.0085	0.0044	0.332×10^{-6}
11.4	1.236×10^{-6}	0.0588	0.0078	0.0041	0.306×10^{-6}
8.1	0.935×10^{-6}	0.0568	0.0068	0.0037	0.281×10^{-6}
5.2	0.651×10^{-6}	0.0546	0.0061	0.0033	0.259×10^{-6}
2.5	0.401×10^{-6}	0.0520	0.0049	0.0028	0.240×10^{-6}

Length=111.9 mm
% Error=11.86

Conclusions

The addition of drainage discs on a vertical fluted tube increased the condensing coefficients of steam by a factor of up to 3.0 compared with that for a fluted tube and up to 6.7 compared with that for a smooth tube. Optimum disc spacing was taken to lie in the range 50–100 mm in the heat flux range 60 000–100 000 W/m² for the tested fluted tube. This range of spacing is also a function of flute geometry, heat flux range and physical properties of the working fluid.

It was shown that an improved version of the hydrodynamic model developed by Somer and Özgen⁶ can be used to predict condensation tube length within $\pm 16\%$ error for a given heat load.

References

1. Williams, A. G., Nandapurkar, S. S. and Holland, F. A. A review of methods for enhancing heat transfer rates in surface condensers. *The Chemical Engineer*, 1968, **233**, CE 367–373

Forthcoming articles

Flow visualisation in a laboratory vaned diffuser

R. B. Brownell, R. D. Flack, M. C. Davis and J. G. Rice

The finite element solutions of laminar flow and heat transfer of air in a staggered or an in-line tube bank

Cha'o-kuang Chen and King-Leung Wong

Maximum size of bubbles during nucleate boiling in an electric field

K. J. Cheng and J. B. Chaddock

An experimental study of the effect of wall temperature non-uniformity on natural convection in an enclosure heated from the side

P. Filis and D. Poulidakos

Laser velocimeter turbulence measurements in shrouded and unshrouded radial flow pump impellers

R. D. Flack and C. P. Hawkins

A one-dimensional model of a thermosyphon with known wall temperature

M. Gordon, E. Ramos and M. Sen

Development of customized shear layers on smooth and rough surfaces

Phillip M. Ligrani

2. Gregorig, R. Haut Kondensation von Feigevellten Oberflächen bei Berücksichtigung der Obertlächenspannungen. *Z. angew. Math. und Phys.*, 1954, **5**, 36–49

3. Combs, S. K. *Experimental Data for Ammonia Condensation on Vertical and Inclined Fluted Tubes*, Oak Ridge National Laboratory Report, Oak Ridge, Tennessee, 1979

4. Mori, Y., Hijikata, K., Hirasawa, S. Nakayama, W. Optimized performance of condensers with outside condensing surface. *Proc. 18th Natl. Heat Transfer Conf., San Diego, California, 6–8 August, 1979*, 55–62

5. Briggs, D. E. and Young, E. H. Modified Wilson-Plot techniques for obtaining heat transfer correlations for shell and tube heat exchanger. *Chem. Eng. Prog. Sym. Series, Heat Trans.*, 1969, **65**(92), 35–45

6. Somer, T. G. and Özgen, C. Hydrodynamics of condensate films on fluted tube surfaces, Part I: Desalination. 1980, **34**, 233–247

7. Özgen, C. *Effect of Tube Surface Geometry on the Rate of Heat Transfer in Desalination by Evaporation*, PhD Thesis, Middle East Technical University, Ankara, 1978

High speed cine observations of cavitating flow in a duct

P. A. Lush and S. R. Skipp

Measurement of streamwise vorticity using a vane vorticity meter

Pan, Huachen and Zhang

The Wells air turbine subjected to inlet flow distortion and high levels of turbulence

S. Raghunathan, T. Seloguchi, K. Kanego and M. Inou

Flow through doubly connected ducts

S. C. Solanki, J. S. Saini and C. P. Gupta

Forced convection heat transfer in doubly connected ducts

S. C. Solanki, J. S. Saini and C. P. Gupta

Developing laminar flow in a semiporous two-dimensional channel with non-uniform transpiration

M. M. Sorour, M. A. Hassab and S. Estafanous

Natural convection on the one side of a vertical wall embedded in a Brinkman-porous medium coupled with film condensation on the other side

A. Voros and D. Poulidakos